2020 IEEE/RSJ International Conference on Intelligent Robots and Systems (IROS)
October 25-29, 2020, Las Vegas, NV, USA (Virtual)

The personalization of stiffness for an ankle-foot prosthesis emulator using Human-in-the-loop optimization

Tin-Chun Wen, Michael Jacobson, Xingyuan Zhou, Hyun-Joon Chung, Myunghee Kim*

***Abstract*—Evidence suggests that the metabolic cost associated with the locomotive activity of walking is dependent upon ankle stiffness. This stiffness can be a control parameter in an ankle-foot prosthesis. Considering unique physical interaction between each individual with below-knee amputation and robotic ankle-foot prosthesis, individually tuned stiffness in a robotic ankle-foot prosthesis may improve assistance benefits. This personalization can be accomplished through human-in-the-loop (HIL) Bayesian optimization (BO). Here, we conducted a pilot study to identify personalized ankle-foot prosthesis stiffness using the HIL BO to minimize the cost of walking, shown by metabolic cost. We used an improved versatile ankle-foot prosthesis emulator, which enabled to test controllers with a wide range of stiffness conditions. Two participants with simulated amputation reduced their cost of walking under the condition of personalized (optimized) stiffness by 6% and 5%, respectively. This result suggests that personalized stiffness may improve assistance benefit.**

Keywords— Ankle-Foot Prosthesis, Stiffness, Metabolic Cost, Bayesian Optimization, Human-in-the-loop

I. Introduction

Individuals with a below-knee amputation usually present a higher metabolic cost, which is typically measured as a respiratory response, when compared to their able-bodied counterparts [1]. Studies have shown that the metabolic cost can be reduced by modifying the mechanical properties of an ankle-foot prosthesis [2-4] such as foot stiffness, perhaps by influencing gait [5-8]. In a simulation study, the improved locomotive performance was achieved in elastic energy storage and return (ESAR) prosthetic foot by stiffening the toe and mid-foot and reducing the stiffness in the ankle and heel [5]. Adjusting the stiffness throughout the different components of the prosthetic foot served to offload the forces experienced by the intact knee and accordingly reduced metabolic cost [5].

*Research partially supported by based on the work supported by the Institute of Civil Military Technology Cooperation funded by the Defense Acquisition Program Administration and Ministry of Trade, Industry and Energy of Korean government under grant No. 19-CM-GU-01.

Tin-Chun Wen is with the Department of Mechanical and Industrial Engineering, University of Illinois at Chicago, Chicago, IL 60607 USA (e-mail: twen9@uic.edu).

Michael Jacobson is with Mechanical and Industrial Engineering Department, University of Illinois at Chicago, Chicago, IL 60607 USA (e-mail: mjacob38@uic.edu).

Xingyuan Zhou is with the Electrical and Computer Engineering Department, University of Illinois at Chicago, Chicago, IL 60607 USA (e-mail: xzhou62@uic.edu)

Hyun-Joon Chung is with the Korea Institute of Robotics and Technology Convergence, Pohang, Korea (e-mail: hjchung@kiro.re.kr).

Myunghee Kim is with Mechanical and Industrial Engineering Department, University of Illinois at Chicago, Chicago, IL 60607 USA (phone: 312-996-3601, e-mail: myheekim@uic.edu)

Such a mechanical parameter in an ankle-foot prosthesis can be personalized. Lower limb prosthesis cannot be a one-size-fits-all design since each user has a unique weight, limb length, leg shape, muscle stiffness, and gait patterns. Therefore, the optimal stiffness profile and the relative control parameters of an ankle-foot prosthesis can be varied depending on the user [5]. A conventional method to tune the stiffness is the weight-dependent method [6]. Higher stiffness is given to a heavier individual. However, such weight-based parameter selection could be inconsistent with a user-preferred parameter [7]. Another potential solution to this parameter selection problem is to utilize a machine learning approach. Such algorithms select a control parameter of an exoskeleton based on the user's performance, given assistance using a selected parameter [2, 3, 8]. The personalization method mostly performed in exoskeletons with healthy individuals, but not in an ankle-foot prosthesis.

Human-in-the-loop (HIL) optimization has been used as a personalization method using a machine learning approach. The algorithm first estimates a cost function from real-time physiological data and then uses this information to determine the optimal, low-cost values for specific control parameters [4, 8-10]. The human-in-the-loop Bayesian optimization has been developed to minimize overall experiment time. This minimal experimental time can be important when physical exertion for prolonged periods is difficult, especially for individuals with impaired mobilities, and also the experimental time can affect the accuracy of the metabolic cost metric [8]. This human-in-the-loop optimization, however, has not been applied for the ankle-foot prosthesis optimization, which may have different user-robot interactions [11, 12].

Such parameter optimization requires a versatile ankle-foot prosthesis testbed, which can present a wide range of torque with high-fidelity [13], [14]. An ankle-foot prosthesis emulator has shown such a capability of high torque, high power, and high control bandwidth [14]. As the human-in-the-loop optimization often accompanies with testing a wide range of parameters during a prolonged period, more robust hardware is essential.

In this study, we explored the importance of the personalized stiffness parameter in an ankle-foot prosthesis by employing an algorithm used in an exoskeleton. For the optimization, we selected ankle-foot prosthesis stiffness, which is a common parameter of a passive ankle-foot prosthesis [11]. Higher number parameter optimization may yield better optimization; however, it increases the experimental time and subsequent fatigue [15], which would be challenging for individuals with impaired mobilities. In the Method section, we first described our robustness improvement on the ankle-foot prosthesis emulator to enable us to test a wide range of stiffness parameters. Then, we

presented our controller implementation, including human-in-the-loop optimization, and then a pilot study with two participants. In section III, we described results and discuss the outcomes.

II. Methods

A. Mechanism:

The two degrees of freedom ankle-foot prosthesis [15] was redesigned and manufactured as an end-effector for a tethered emulator system (Fig.1). The ankle-foot prosthesis is composed of a frame, two toes, and a compliant heel. The main body of the ankle-foot prosthesis (including the toes and frame) consists of 7075-T6 aluminum and was machined with a computer numerical control (CNC) method. Contained within the frame are needle bearings, which are press-fit, allowing two notched shafts to rotate about the same axis. Each shaft is then fixed to a single toe by the use of a set screw. The rotation of each shaft-toe assembly is similar to the dorsiflexion and plantarflexion of a human ankle joint. A heel spring machined of fiberglass provided from Gordon Composites is attached to a transverse surface of the frame.

The ankle-foot prosthesis emulator operates based on angle and torque to generate plantar-dorsiflexion movement. Plantarflexion is conducted when the heel spring makes ground contact and when toe structures produce push-off from motor actuation. This emulator can adjust ankle stiffness through motor torque output based on ankle angle (Fig. 2).

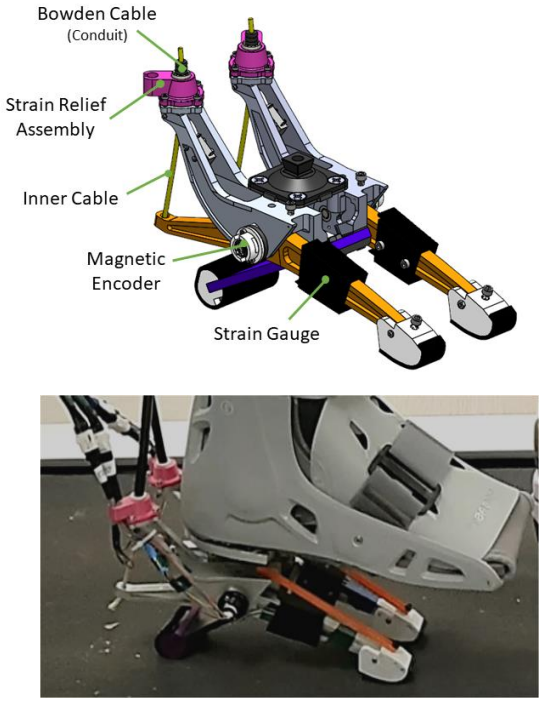

Figure 1. Mechanism of the Ankle-foot prosthesis end-effector: (Top) CAD model with detailed description, and (Bottom) Hardware implementation. We printed strain relief assembly, toes (white part), etc. We improved the robustness of the heel (purple part) using carbon fiber. Pulling the inner cable provided plantarflexion, releasing the inner cable and using rubber bands between screws on toes and the main part was for dorsiflexion.

The redesign consisted of an improved Bowden cable strain relief assembly, which utilizes Thermoplastic Urethane (TPU) inserts. The improved assembly allows for reduced maintenance during walking trials by holding Bowden cables in place without a setscrew. The use of 3D printed polymers also reduces overall device weight by approximately 0.10 kg.

Torque and angular data are processed by sensors to produce ankle-foot prosthesis movement using encoders (U.S. Digital MAE-5 Encoders), and strain gauges (Omega), respectively. All sensors are packaged within newly designed Fused Deposition Modeled (FDM) enclosures to prevent damage during walking trials. FDM pads with rubber surfaces are attached to each toe and heel spring which serve to increase ground traction.

Motors from Humotech Caplex Actuator Units (Humotech, Pittsburgh, USA) emit torque values restricted to a peak of 180N-m for ankle-foot prosthesis emulator application. Powerful actuation and control hardware is located off-board to keep worn mass low. Flexible Bowden cable tethers transmit mechanical power to the prosthesis but do not interfere with the natural movements of the limb. Bowden cables exert transmitted torque to the ankle-foot prosthesis for movement. As a pulley rotates from the actuator units, the conduit of the Bowden cables exerts an equal and opposite reaction to reduce any net force experienced by the end-effector itself. The inner cables of the Bowden cable then pull upward on the posterior aspect of each toe as the opposite end contacts the ground to generate a moment. This moment results in plantarflexion of the ankle-foot prosthesis. Also, during the swing phase, when torque from the actuator units is at a minimum, rubber bands act to dorsiflex each toe.

Multiple preliminary tests were conducted to validate ankle-foot prosthesis torque control robustness before optimization testing. These tests included sensor calibration, bench-top step frequency control, and one degree of freedom walking [15].

B. Controller

The controller was composed of three layers: low-level, mid-level, and high-level controller. The low-level controller controlled ankle-angle position, motor position, motor velocity, and torque.

The mid-level controller was a walking controller based upon gait mechanics. We divided gait into two phases: swing and stance phases. The stance phase was further divided into dorsiflexion and plantarflexion. During the swing phase, we conducted ankle-angle position control. During the stance phase, we executed torque control. In the mid-level controller, it generated an ankle-angle torque curve using an optimizable stiffness parameter (Fig 2). Changing the stiffness parameter influenced the peak torque and shape of the ankle-angle torque curve. The desired torque, in the stance phase, was determined from ankle-angle torque based on ankle-angle.

As a comparison, we also employed a control-off condition during walking. In this mode, motor position control was conducted. Therefore, the toes could only move slightly due to the elasticity of the ropes during walking.

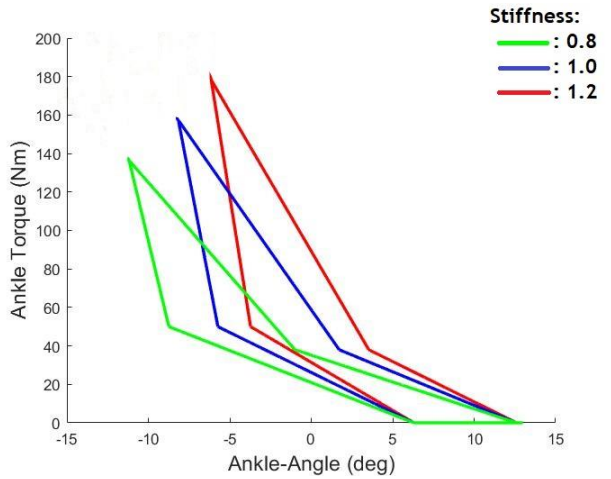

Figure 2. Ankle-angle Desire Torque Curve in different stiffness values. Stiffness influenced the peak torque and angle, and also the shape of the ankle-angle torque curve. Higher stiffness resulted in higher torque.

The swing, dorsiflexion, and plantarflexion were detected using ankle angle, torque, and power. In the swing phase, ankle torque should be close to zero and ankle-angle should be higher than 0 degrees. In the stance phase, actual torque should be higher than 5 N-m, and ankle-angle should not exceed 15 degrees. Plantarflexion occured when the angular velocity became zero at high torque.

The high-level controller is an optimization controller. It conducted the Bayesian Stiffness parameter optimization using a cost function of the metabolic cost [16]. The optimization identified the next parameter and sent back to the mid-level controller to generate an ankle-angle torque curve. The new curve was used to command the desired torque of low-level control.

C. Human-in-the-loop Bayesian Optimization

Bayesian optimization is a sequential design strategy for near-global optimization of the black-box function. In Bayesian optimization, given observed set of data, a new parameter is selected x_* [17]. These predictions are then used in a search for a minimum parameter of the unknown objective function, f [18].

Firstly, a probability was set prior to the optimization, which means that the hyperparameters were initialized with a "best guess" with an assumption that the collected data would follow a normal distribution with zero mean and covariance of σ_n^2 [17]. The covariance function, which encodes the assumptions of the unknown objective function that we try to minimize, was selected based on our domain knowledge. For our experiment, we selected the squared exponential kernel, given by (2), as a covariance function [17].

$$k(x_i, x_j) = \sigma_f^2 \exp\left(-\frac{1}{2l^2}(x_i - x_j)^2\right) + \sigma_{noise}^2 \delta_{ij} \qquad (2)$$

The hyper-parameters of this covariance function, expressed as a vector θ, was continuously optimized by maximizing the log marginal likelihood, as given by (3). The noise hyperparameter, σ_{noise}, included measurement noise from the respiratory measure and uncertainty due to fatigue or short-term adaptation. This optimization process employed constrained nonlinear programming to iteratively evaluate the log-likelihood through the use of a Cholesky decomposition of the covariance matrix, *K*, and the derivative of the log-likelihood [17].

$$\max_{\theta} \log(y \mid X, \theta) \qquad (3)$$

The kernel function was used to calculate the Gaussian Process (GP) regression, which contributed a posterior distribution that related the dependent variable, metabolic cost, to the stiffness parameter, including uncertainty from the measurement noise. The posterior mean and covariance were calculated by Gaussian Process through the computation of the covariance matrix *K*, given by (4), the vector of covariances *k* between the unseen value, x_*, and the observed data, given by (5).

$$\boldsymbol{K} = \begin{pmatrix} k(x_1, x_1) & \cdots & k(x_1, x_n) \\ \vdots & \ddots & \vdots \\ k(x_n, x_1) & \cdots & k(x_n, x_n) \end{pmatrix} \qquad (4)$$

$$\boldsymbol{k} = [k(x_*, x_1), k(x_*, x_2), \ldots, k(x_*, x_n)] \qquad (5)$$

The predicted mean and covariance for the distribution containing the observed data and the unseen data point x_* are given by (6) and (7), respectively.

$$\mu_n(x_*) = \boldsymbol{k}^T \boldsymbol{K}^{-1} \boldsymbol{y}_{1:n} \qquad (6)$$

$$\sigma_n^2(x_*) = k(x_*, x_*) - \boldsymbol{k}^T \boldsymbol{K}^{-1} \boldsymbol{k} \qquad (7)$$

The next control parameter was selected by using the acquisition function using the predicted mean and covariance functions from Gaussian Process [19]. We used Expected Improvement (EI) as an acquisition function, which balances exploitation and exploration [8] based on our previous study [8], where we found that the exploration-focused Upper Confidence Bound method would increase experimental time, especially with high measurement uncertainty. The next parameter, x_{*+1}, from EI was evaluated (y_{*+1}), and then added to the observed dataset *D*.

$$EI[x_*] = (f_{best} - \mu_*)CDF(u_*) + \sigma_* PDF(u_*) \qquad (8)$$

$$u_* = \frac{(f_{best} - \mu_*)}{\sigma_*} \qquad (9)$$

μ_* : mean CDF: Cumulative distribution function.

σ_* :Standard Deviation PDF: Probability density function.

In our experiment, we initialized the Bayesian optimization using four randomly selected parameters, stiffness, in each bin of 1.25-1.5, 1-1.25, 0.75-1, and 0.5-0.75. The range of the stiffness was 0.5 to 1.5. Then, we repeated the process of calculating posterior distribution using obtained data, parameter selection using EI, and evaluation until eight number of iterations (Fig. 3). For each iteration, we

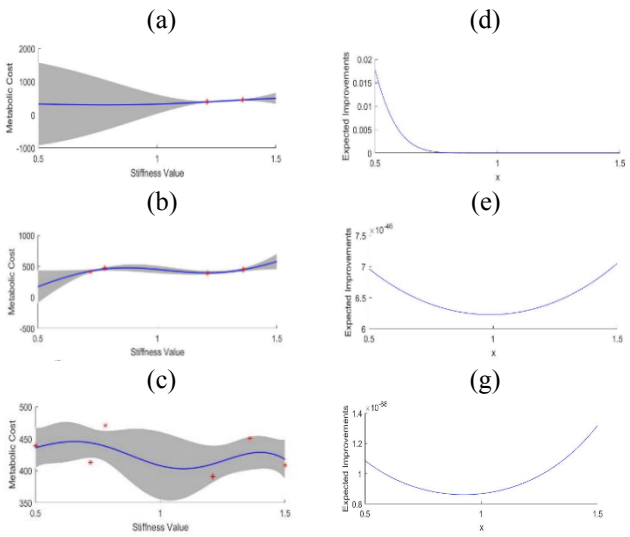

Figure 3. Process of the Bayesian Optimization of 2nd, 4th,and 7th iterations (top, middle, bottom, respectively). (a-c) Posterior distribution and (d-g) expected improvement. The red stars are collected data, the blue line is the estimated value and the gray area is the standard deviation;)

collected about 30 breaths, which took approximately two minutes. The number of iterations was decided by visually investigating the change in the mean distribution with uncertainty from the noise measurement.

We used cost function (f^{inst}) directly from the respiratory measure, z. The metabolic rate was predicted by fitting a first-order dynamic model of 2 min respiratory data using the equation (10) [9].

$$z(j+1) = \frac{(\tau - dt(j))}{\tau} z(j) + \frac{dt(j)}{\tau} + f^{inst} \qquad (10)$$

where j is subject breath's index and dt(j) is the time continuation between jth breath and (j+1)th breath.

Using measured z and dt for 2 min, f^{inst} was estimated using the instantaneous cost mapping method which employed the least-squares to minimize the error between the measurements and model estimation [20].

D. Experiment Protocol

We tested the feasibility of the individualization by conducting a pilot study with two individuals with simulated amputation (male, Age: 26, 27, Height 173, 179 cm, Weight: 71, 84 kg). The overall structure of the system is shown in Fig 4. We estimated the cost of walking by measuring respiratory rate (Cosmed K5, Rome, Italy). The Cosmed K5 sensed velocity (L/min) of oxygen and carbon dioxide in the subject's breath.

	Conditions	Time
1	Standing	3 mins
2	Control-off	5 mins
3	Bayesian Optimization	12 mins
4	Worst Condition	5 mins
5	Best Condition	5 mins
6	Control-off	5 mins
7	Normal Walking	5 mins

Table 1. Experiment Protocol

Table 1 shows our human subject experiment protocol. The experiment started from the standing condition and control-off mode (holding the motor). We used Human-in-the-loop Bayesian optimization method to find the worst and best stiffness conditions for each subject. After the HIL Bayesian optimization session, we provided the worst and best conditions to verify the HIL Bayesian optimization results. In the end, control-off mode and normal walking conditions were presented to compare to the other conditions. In between walking trials, the subject had 5-minute breaks.

For the best, worst, and control-off conditions, we calculated and compared the metabolic cost (Met) with the formula (equation 11) [21] using the last two-minute data of five-minute walking:

$$Met = (16.58 * VO_2 + 4.5 * VCO_2)/60 \qquad (11)$$

Where, VO_2 is the velocity of oxygen and VCO_2 is the velocity of carbon dioxide.

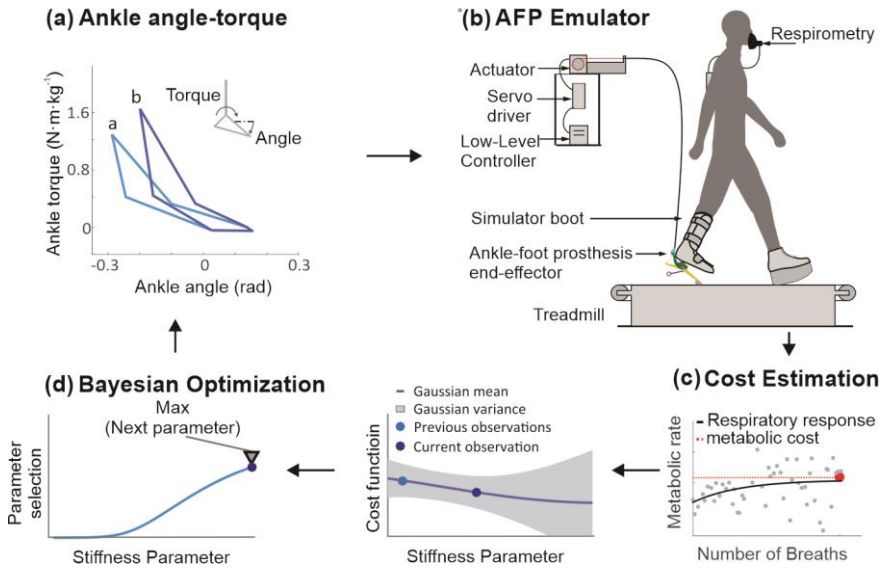

Figure 4. Human-in-the-loop Bayesian optimization of AFP stiffness parameter. **(a)** desired torque was decided depending on the user's ankle angle, and the torque was sent to the ankle-foot prosthesis emulator. **(b)** the low-level controller conducted torque control to meet the desired torque and the user walked on a treadmill. **(c)** The measured respiratorty rate data were used to estimate the metabolic cost. **(d)** Bayesian optimization calculated the posterior distribution and selected the next stiffness parameter. The stiffness parameter decided the desired ankle torque curve (**(a)**).

In general, the participants walked 0.9 m/s, a self-selected comfortable speed. During optimization, we provided adaptation time to a participant by slowing down the speed for one minute when the condition changed. For the first 30 seconds, the participant walked at 0.45 m/s and then at 0.675 m/s during the following 30 seconds, and 0.9 m/s for the last minutes. To be consistent, we also provided similar adaptation periods to other conditions. Subjects were also allowed to have enough break time to recover from fatigue under the controlled environment such as sound and light.

III. Results and Discussion

A. Ankle-foot prosthesis emulator – tracking performance

The ankle-foot prosthesis emulator presented a wide range of torques with small tracking errors (less than 1% compared to peak torque for all conditions) (Fig 5a, c, e, g). For the error, we used the RMS (Root Mean Square) error between desired torque and actual torque using the last two minutes' data, which contained approximately 100 steps. The emulator also showed a wide range of motion in ankle angle (Fig 5a, b, e, f), and provided high power up to 1 kW (Fig 5d, h). These characteristics made it ideal for this device to test the importance of personalization through human-in-the-loop Bayesian Optimization.

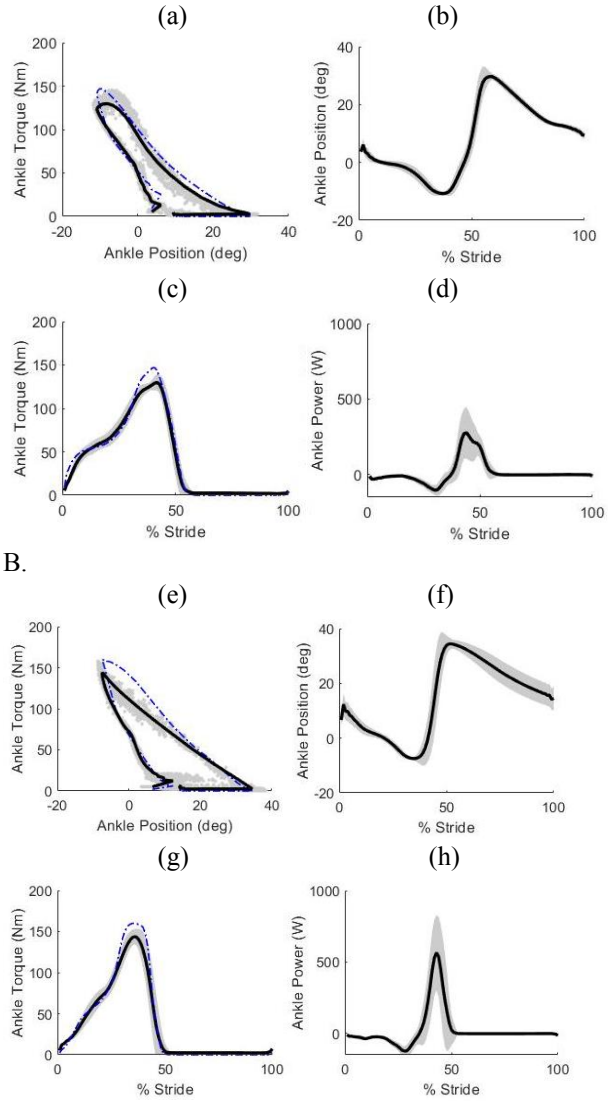

Figure 5. Ankle angle-torque mechanics for the best condition. (A) subject 1 (stiffness = 1.15) and (B) subject 2 (stiffness = 1.5). In the figures, we showed the desired torque (blue line), mean value (black line), and standard deviation (grey area). Each of A) and B) presents four curves, ankle-angle torque curves (a, e), ankle position (b, f), ankle torque tracking performance (c, g), and ankle power (d, h).

B. Personalized stiffness using HIL Optimization

The optimal stiffness was vastly different between the two subjects, which resulted in different ankle angle torque curves and power curves (Fig 5). The best stiffness parameter was 1.15 and 1.5 for the participants 1 and 2, respectively. For the best conditions, the participant 1 and 2 reduced their cost of walking by 5% and 6% on average compared to the control-off condition (Fig. 6). The worst parameters were 0.85 and 0.5 for participants 1 and 2, respectively, and the participants increased the metabolic cost by 3% and 1%, respectively (Fig. 6). This result is similar to the outcome from the metabolic cost landscape, depending on the stiffness conditions (Fig. 7).

In addition, both of the personalized parameters were different from the weight-based parameter, which was about 0.9 for participant 1 and 1 for participant 2. These parameter sets actually could increase the cost of walking. This result suggests that personalized assistance can be useful to maximize assistance benefits. Rigorous investigation with an increased number of participants would clearly reveal the importance of personalization.

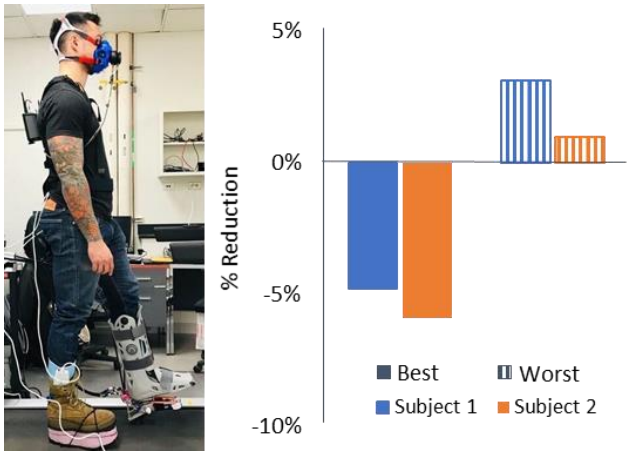

Figure 6. Left: Experimental setup. Right: Metabolic Cost Reduction for subject 1 (blue) and subject 2 (orange), for the conditions of best personalized stiffness (solid fill) and worst personalized stiffness (dashed fill), compared to the powered-off condition. The personalized stiffness greatly reduced the cost of walking for two participants.

IV. Conclusion

We conducted a pilot study to test the importance of personalized assistance in ankle-foot prosthesis with individuals with simulated amputation, motivated by the previous studies on the exoskeleton. For this study with an ankle-foot prosthesis, we improved our previous ankle-foot prothesis emulator for the purpose of robustness improvements and employed human-in-the-loop Bayesian

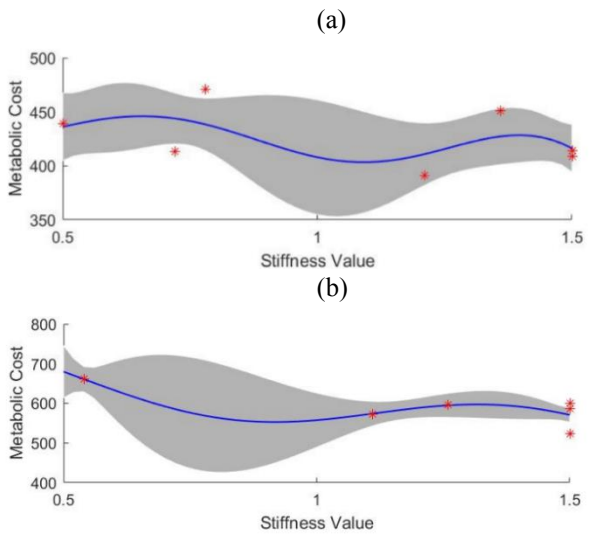

Figure 7. Metabolic cost landscape of subject 1 (a) and 2 (b). The blue lines are the mean metabolic cost curve, and gray areas indicate the uncertainty of the curve. The red star indicates the collected data.

optimization to personalize ankle-foot prosthesis parameters. The improved emulator enabled us to continuously conduct an experiment more than twenty minutes while tracking the desired torque with minimum error. Compared with the weight-based parameters, the predictive mean of Gaussian processes at optimized parameters was lower. The pilot study shows that the optimization helped to identify the optimal stiffness parameter set, which reduced the cost of walking. Future work will include a systematic investigation of the stiffness optimization in ankle-foot prosthesis emulator with a refined experimental protocol for a rigorous comparison to the weight-based parameter. Another direction would be investigating the effect of the personalization on the physical effort using other clinically relevant parameters with an advance in optimization speed. We will also investigate other related cost function, such as socket interface pressure [22].

ACKNOWLEDGMENT

The authors thank Seongmi Song for her contribution to an experimental protocol, Prakyath Kantharaju and Anchi He for their contribution to the system development, and Christopher on their contribution to the hardware development.

REFERENCES

[1] S. K. Au, J. Weber, and H. Herr, "Powered Ankle--Foot Prosthesis Improves Walking Metabolic Economy," IEEE Trans. Robot., vol. 25, no. 1, pp. 51–66, Feb. 2009.

[2] J. Zhang, P. Fiers, K. A. Witte, R. W. Jackson, K. L. Poggensee, C. G. Atkeson, and S. H. Collins. Human-in-the-loop optimization of exoskeleton assistance during walking, Science 356(6344), 1280-1284.

[3] M. Kim†, C. Liu†, J. Kim, S. Lee, A. Meguid, C. J. Walsh, and S. Kuindersma, Bayesian optimization of soft exosuits using a metabolic estimator stopping process, International Conference on Robotics and Automation, 2019 († equal contributor).

[4] J. R Koller, D. H Gates, D. P Ferris, and C. David Remy, "'Body-in-the-Loop' Optimization of Assistive Robotic Devices: A Validation Study," in Robotics: Science and Systems XII.

[5] N. P. Fey, G. K. Klute, and R. R. Neptune, "Optimization of Prosthetic Foot Stiffness to Reduce Metabolic Cost and Intact Knee Loading During Below-Knee Amputee Walking: A Theoretical Study," J. Biomech. Eng., 2012.

[6] M. Kim and S.H. Collins, Once-per-step control of ankle-foot prosthesis push-off work reduces effort associated with balance during walking, Journal of Neuroengineering and Rehabilitation, 12:43, 2015

[7] M. Kim and S. H. Collins, Step-to-step ankle inversion/eversion torque modulation can reduce effort associated with balance, Frontiers in Neurorobotics, 11: 62, 2017.

[8] M. Kim et al., "Human-in-the-loop Bayesian optimization of wearable device parameters," PLoS One, vol. 12, no. 9, p. e0184054, Sep. 2017.

[9] W. Felt, J. C. Selinger, J. M. Donelan, and C. D. Remy, "'Body-In-The-Loop': Optimizing Device Parameters Using Measures of Instantaneous Energetic Cost," PLoS One, vol. 10, no. 8, p. e0135342, Aug. 2015.

[10] J. Zhang et al., "Human-in-the-loop optimization of exoskeleton assistance during walking.," Science, vol. 356, no. 6344, pp. 1280–1284, Jun. 2017.

[11] J. M. Caputo and S. H. Collins, "Prosthetic ankle push-off work reduces metabolic rate but not collision work in non-amputee walking.: Scientific reports, vol. 4, p. 7213. 2014

[12] R. W. Jackson and S. H. Collins, "An experimental comparison of the relative benefits of work and torque assistance in ankle exoskeletons.", Journal of applied physiology, vol. 119, no. 5, pp. 541-557. 2015.

[13] J. M. Caputo and S. H. Collins, "Prosthetic ankle push-off work reduces metabolic rate but not collision work in non-amputee walking," Sci. Rep., vol. 4, no. 1, p. 7213, May 2015.

[14] S. H. Collins, M. Kim, Tianjian Chen and Tianyao Chen, "An ankle-foot prosthesis emulator with control of plantarflexion and inversion-eversion torque," 2015 IEEE International Conference on Robotics and Automation (ICRA), Seattle, WA, 2015, pp. 1210-1216.

[15] M. Kim, T.Chen, T.Chen, and S.H.Collins, An ankle foot prosthesis emulator with control of plantarflexion and inversion-eversion torque, Transactions on Robotics, 99: 1-12, 2018.

[16] Jonas Mockus (2012). Bayesian approach to global optimization: theory and applications. Kluwer Academic.

[17] C. E. Rasmussen and C. K. I. Williams, Gaussian processes for machine learning. MIT Press, 2006.

[18] B. Shahriari, K. Swersky, Z. Wang, R. P. Adams, and N. de Freitas, "Taking the Human Out of the Loop: A Review of Bayesian Optimization," Proc. IEEE, vol. 104, no. 1, pp. 148–175, Jan. 2016.

[19] J. Snoek, H. Larochelle, and R. P. Adams, "Practical Bayesian Optimization of Machine Learning Algorithms," pp. 1–9.

[20] YeDing ,Myunghee Kim Human-in-the-loop optimization of hip assistance with a soft exosuit during walking Sci. Robotics 3, eaar5438

[21] ALBERTO RUIZ AND NESTOR W. SHERMAN, An Evaluation of the Accuracy of the American College of Sports Medicine Metabolic Equation for Estimating the Oxygen Cost of Running, Journal of Strength and Conditioning Research: August 1999 - p 219-223

[22] Sebastian I. Wolf, Merkur Alimusaj, Laetitia Fradet, Johannes Siegel, Frank Braatz (Dec 2009) Pressure characteristics at the stump/socket interface in transtibial amputees using an adaptive prosthetic foot

[23] Roberto E.Quesada, Joshua M.Caputo, Steven H.Collins, Increasing ankle push-off work with a powered prosthesis does not necessarily reduce metabolic rate for transtibial amputees, 3 October 2016